TGA-FTIR Analysis of Torrefaction of Lignocellulosic Components (cellulose, xylan, lignin) in Isothermal Conditions over a Wide Range of Time Durations

Pin Lv,[a] Giana Almeida,[b] and Patrick Perré [a,*]

This study investigated chemical decomposition of lignocellulosic components in the course of torrefaction under isothermal conditions for durations up to 5 hours. The goal was a better understanding of the behaviour of biomass, at both short and long residence times, which is important for innovation in the chemical and bioenergy industries. Gaseous and solid-phase decomposition products of cellulose, xylan, and two lignins, were studied following torrefaction at three temperatures (220, 250, and 280 °C) for a continuous recording of mass loss and emission of volatiles over 5 hours. Two decomposition stages were revealed for xylan, with a notable release of CO that increased with treatment temperature. 4-O-methyl glucurono-units on the side chains of xylan degraded first, and acetyl groups and macromolecule fragments accounted for the second degradation, starting at 250 °C. The primary production of acetic acid occurred at 280 °C. For the two lignins, decomposition reactions predominated at lower temperatures, while rearrangement prevailed at 280 °C. The emission of phenol was a clear distinction between the two. Cellulose was thermally stable at short times under all treatments, but it decomposed dramatically afterwards, especially at 280 °C.

INTRODUCTION

Pyrolysis of wood and its components to produce fuels and chemicals, as well as the specific characterisation of feedstock materials, has been investigated under various conditions. Gas chromatography (GC), gas chromatography-mass spectrometry (GC/MS), thermogravimetry (TGA) coupled with Fourier transform infrared spectroscopy (FTIR), and pyrolysis-GC-FTIR techniques at temperatures up to 900 °C have been used to characterise the pyrolytic mechanisms of cellulose, xylan, and lignin (Biagini *et al.* 2006; Yang *et al.* 2007; Shen and Gu 2009; Wu *et al.* 2009; Shen *et al.* 2010a,b; Qu *et al.* 2011). Moreover, kinetic models to predict the pyrolysis behaviour of biomass have been developed. The key to modelling lies in understanding the complex degradation behaviour of lignocellulosic components in both the solid and gas phases.

Compared to pyrolysis, torrefaction, a treatment at lower temperature (in the range of 200 to 280 °C), can increase the energy density of wood and is a feasible pre-treatment for biofuel production. Studies of torrefaction have focused on the interaction between temperature and duration to optimise their effects for the purpose of energy production (Rousset *et al.* 2009, 2011). Considering the large amount of biomass to be treated at the industrial level for bio-fuel production, there is an incentive to work at high temperature to

shorten the process duration. Moreover, another issue of concern involves the large amount of biomass to be treated, which may have quite long heating and cooling time depending on the process design, which can induce longer actual treatment durations than initially expected (Cavagnol *et al*. 2015). Accordingly, the knowledge of torrefaction over a wide range of temperature levels and for both short and long time-durations is crucial. However, few studies have examined the thermochemical properties of the reaction products under these conditions.

In the present study, torrefaction of cellulose, xylan, and two lignins (extracted from spruce and poplar) was conducted at 220, 250, and 280 °C by TGA for a continuous recording of mass loss and emission of volatiles over 5 h. The release of gaseous products was monitored simultaneously using an on-line FTIR gas cell, and changes in the solid phase were determined using attenuated total reflectance (ATR) of FTIR. The results include a detailed characterisation of the effect of torrefaction temperature and the range of time-duration on the chemical breakdown products of the lignocellulosic components. Key insights were revealed regarding the reaction mechanisms that take place during the torrefaction of biomass.

EXPERIMENTAL

Materials

Microcrystalline cellulose (Product No. 310697) and xylan extracted from beech wood (Product No. X4252) were obtained from Sigma-Aldrich, France. Milled wood enzyme lignin (MWEL) fractions were prepared from extract-free spruce (*Picea abies*) and poplar (*Populus euramericana*, cv I214) woods using a previously described method (Lapierre *et al.* 1986). In this work, LS and LP are abbreviations for lignin from spruce and poplar, respectively.

All samples were subjected to elemental analysis three times using Flash 2000 CHNS/O Analyzers (Thermo Scientific) on a dry basis. The results are shown in Table 1.

Table 1. CHNS/O Determination (Dry basis)

	C (wt. %)	H (wt. %)	O (wt. %)	N (wt. %)	S (wt. %)
Cellulose	43.22	6.0	47.79	0	0
Xylan	41.15	5.42	41.45	0	0
LS	58.68	5.53	29.27	0	0.5
LP	55.43	5.45	32.77	0	1.07

TGA

Samples weighing approximately 10 mg were placed in open, 70-μL aluminum crucibles and heated with a TGA-DSC 1 apparatus (Mettler®, France) from ambient temperature to 110 °C at a heating rate of 5 °C/min. The samples were then dried for 30 min at 110 °C. The mass recorded at the end of this drying segment was considered the initial mass to determine the mass loss by torrefaction. Following drying, the temperature was increased by 5 °C/min until the final temperature (220, 250, or 280 °C) was reached. The final temperature was maintained for 5 h. All treatments were performed in a nitrogen atmosphere with a gas flow of 50 mL/min. At least three tests were carried out for each

condition, and the TGA curves presented in this work show data after the blank was subtracted. The mass loss (ML) of the sample was calculated using the following equation,

$$ML= [(M_0 - M_t)/ M_0] \times 100\% \qquad (1)$$

where M_0 is the weight at the end of drying and M_t is the weight after torrefaction.

The TGA curves presented in this work were collected after the drying segment, and the mass losses are listed in Table 2.

Table 2. Mass Loss of Samples during the Treatment

Treatment		Mass loss %			
		Xylan	LS	LP	Cellulose
220 °C	110 °C < T < 220 °C (22 min)	5.7	3	5	0.3
	10 min	12.2	6.5	9.7	0.5
	30 min	15.9	8.7	13.4	0.9
	1 h	19.3	10.2	16.4	1.3
	2 h	24.2	11.7	19.1	2
	5 h	33.3	13.9	22	3.5
250 °C	110 °C < T < 250 °C (28 min)	17.5	8.4	11.9	1
	10 min	28.5	13.1	19.5	3.1
	30 min	36.8	15.8	24.3	5.7
	1 h	42.6	17.7	26.9	9.1
	2 h	47.8	19.2	29	15.4
	5 h	53.9	21.1	31.2	33.1
280 °C	110 °C < T < 280 °C (34 min)	35.8	15.2	21.8	4.1
	10 min	49.4	20.5	29.6	13.5
	30 min	53.2	23.5	33.8	31.8
	1 h	55.1	25.3	35.7	53
	2 h	56.7	26.7	37.3	74.4
	5 h	58.2	28.5	39.2	84.4

TGA-FTIR

A TGA device was coupled with a Nicolet™ 6700 (Thermo SCIENTIFIC, USA) infrared spectrometer through FTIR/TA interface transfer equipment with a 10-cm gas cell. The transfer line and gas cell were maintained at a temperature 10 °C higher than that of the torrefaction treatment to prevent condensation. The gas flow rate through the transfer line and gas cell was kept constant. Infrared spectra over the range of 4000 to 650 cm^{-1} were collected every 15 s at a resolution of 4 cm^{-1}.

During TGA operation, the evolving gas products were transported out of the furnace directly into the gas cell, where the volatiles were analysed by an FTIR gas spectrometer. The absorption bands of each spectrum collected are simultaneously integrated over the entire spectral range. Gram-Schmidt curves are obtained by plotting this integration from each spectrum as a function of time. These curves were used to have an overview of volatiles production throughout the test. Times of interest can subsequently be chosen for a detailed analysis of the spectra. This allowed us to identify the dominant volatiles from the corresponding torrefaction process as shown in Table 3.

FTIR-ATR

Residues remaining after the TGA test, along with untreated samples, were examined for solid phase changes using a Nicolet 6700 apparatus combined with an ATR unit (SMART, iTR, Thermo SCIENTIFIC, USA) at a resolution of 4 cm^{-1} for 64 scans in the range from 4000 to 650 cm^{-1}. Samples were pressed against the diamond crystal of the ATR device. A pressure applicator with a torque knob ensured that the pressure applied was the same for all measurements. A background spectrum was recorded prior to each test spectrum. A reference compilation of the products identified by infrared analysis in previous studies was generated. In addition, the infrared spectra of several wood component monomers obtained from the NIST (National Institute of Standards and Technology, USA) and AIST (National Institute of Advanced Industrial Science and Technology, Japan.) databases also were used as references.

RESULTS AND DISCUSSION

Xylan

Xylan exhibited poor thermal stability and decomposed rapidly, resulting in mass losses of 12.2 and 28.5% during the period following drying up until 10 min of torrefaction at 220 and 250 °C, respectively (Table 2; Fig. 1). After 5 h, mass losses were 33.3 and 53.9% at 220 and 250 °C, respectively. Xylan underwent a rapid initial period of decomposition that resulted in a mass loss of 49.4% up until 10 min of torrefaction at 280 °C, but levelled off thereafter, with only 9% additional mass loss during the remainder of the treatment.
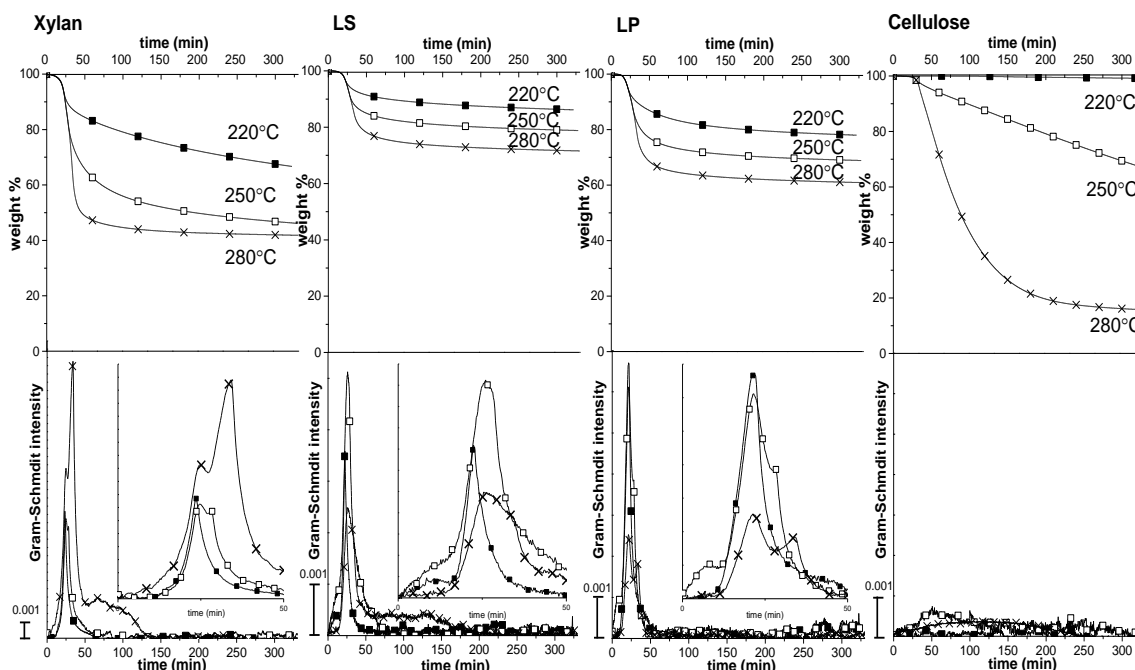

Fig. 1. Mass loss and Gram-Schmidt curves of torrefied samples. The upper graphs represent mass loss, and the lower graphs indicate G-S intensity (an intensity of 0.001 scale bar is provided; partial magnified graphs are embedded). The line with solid squares is for torrefaction at 220 °C; the line with hollow squares is for torrefaction at 250 °C; the line with crosses is for torrefaction at 280 °C.

The average intensity of volatiles during the mass loss was determined and depicted in the Gram-Schmidt (G-S) curves based on vector analysis. As can be seen in Fig. 1, maximum volatiles production occurred within a short time period at the beginning of each torrefaction, indicating that decomposition occurred rapidly once the final temperature was reached. Moreover, the intensity of the G-S peak increased with increasing temperature. An interpretation of two successive G-S peaks observed at 250 and 280 °C suggests that there were two distinct degradation steps, in agreement with the findings of Di Blasi and Lanzetta (1997). The two steps occurred following drying: the first step was fast and resulted in a large release of volatiles, while solid residue degradation yielded the second release of volatiles when the final temperature was reached.

Three-dimensional (3D) infrared diagrams were obtained simultaneously through TGA-FTIR, providing clear pictures of the volatiles evolved from xylan (Fig. 2a). Spectra at the maximum evolution rate in each 3D spectrogram were separated and are presented in Fig. 2b. At 220 °C, water (3450 to 4000 cm^{-1}; 1300 to 1590 cm^{-1}), CO_2 (2240 to 2390 cm^{-1}), formic acid (3450 to 3650 cm^{-1}; 1710 to 1850 cm^{-1}; 1030 to 1150 cm^{-1}), methanol (3600 to 3700 cm^{-1}; 2700 to 3100 cm^{-1}; 900 to 1100 cm^{-1}), and small amounts of CO (2040 to 2240 cm^{-1}) were observed. During torrefaction at 250 °C, the characteristic bands of the two G-S peaks were similar to those at 220 °C but exhibited stronger CO_2 and CO peak intensities. Moreover, closer inspection of the two spectra illustrated that the intensity of the formic acid peak was reduced in the second G-S peak. In addition, acetic acid (3500 to 3650 cm^{-1}; 1650 to 1870 cm^{-1}; 900 to 1480 cm^{-1}) was identified in both spectra at 250 °C. More volatiles evolved during torrefaction at 280 °C: the spectrum from the first G-S peak showed little difference to that at 250 °C, while the spectrum from the second G-S peak revealed remarkable production of CO_2, CO, and acetic acid. From Figs. 2a and 2b, it can be concluded that the second step of xylan decomposition began at 250 °C and that the main production of acetic acid occurred at 280 °C.
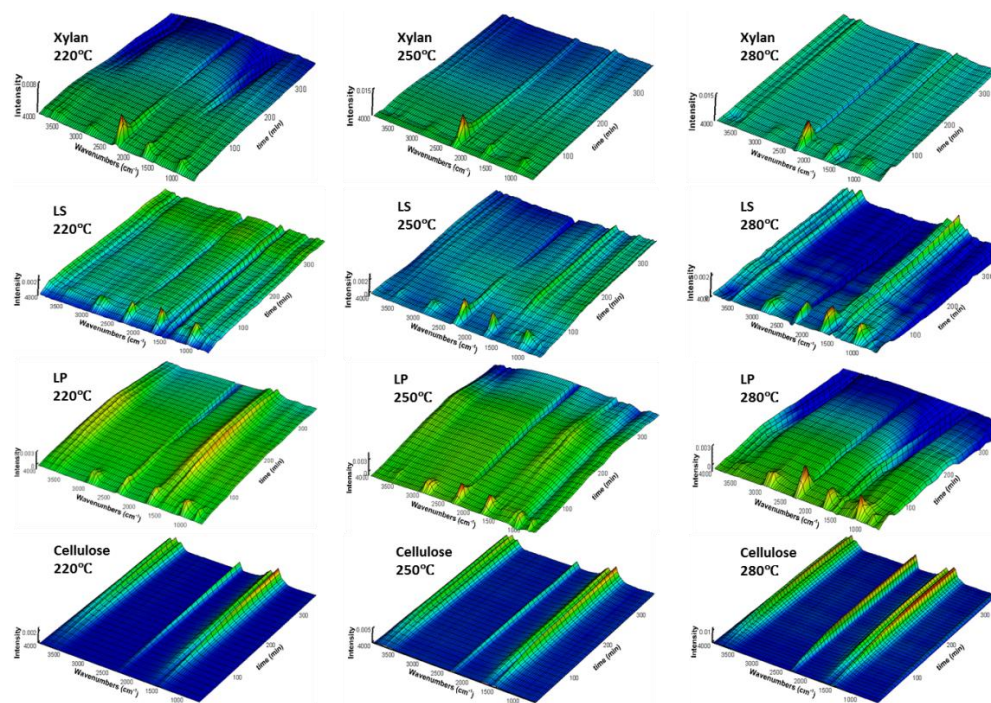

Fig. 2a. 3D spectrograms of volatiles from torrefied samples

Figure 3 shows the FTIR-ATR spectra of the residues in the solid phase. Absorptions above 3200 cm^{-1} were associated with O-H stretching vibrations, while stretching vibrations of C-H occurred at 3000 to 2800 cm^{-1}. The O-H absorption intensity decreased with increasing torrefaction temperature, while C-H absorption intensity decreased at 220 °C but increased at 250 and 280 °C, suggesting that xylan initially dehydrated/dehydrogenated and underwent subsequent rearrangement at higher temperatures. In contrast to the high degree of spectral similarities in the wavenumber range from 3700 to 2800 cm^{-1}, great differences occurred in the fingerprint region (1800 to 650 cm^{-1}), in which the characteristic peaks of xylan included 1725 (v C=O), 1601 (v COO$^-$, asym), 1460 (δ CH$_3$ asym. in methoxy), 1407 (v COO$^-$, sym plus δ –CH$_2$–C=O in carboxylic acids), 1382 (δ CH$_3$ sym. in acetate), 1312 (v COO$^-$, sym / δ CH; δ OH), 1250 (δ O-H plus CO-O in acetate), 1212 (v C-O-C in acetate ester), 1163 (v bridge C-O-C), 1110 (cyclic ether, asym), 1079 (C-O in carboxylic acid), 1038 (v C-O in alicyclic secondary alcohols, six-membered ring), 982 (δ OH, ring), 895 (δ CH, C-O-C, sym.), 843 (δ COO$^-$), and 780 cm^{-1} (δ COO$^-$), as shown in the enlarged graph in Fig. 3 (Marchessault and Liang 1962; Kačuráková *et al.* 1999). COO$^-$ groups were detected in untreated xylan (Buslov *et al.* 2009). After torrefaction at 220 °C for 5 h, asymmetric and symmetric stretching and deformation vibrations of COO$^-$ absorptions shifted and the pronounced peaks at 1589, 1400, 843, and 780 cm^{-1} demonstrated the formation of new carboxylic acid salts (Shevchenko 1963). Moreover, the decrease of the peak intensities at 1382, 1250, 1460, and 1407 cm^{-1} suggested the decomposition of 4-O-methyl glucurono-units in the side chains, leading to the production of carbonyls and H$_2$O, CO$_2$, formic acid, methanol, and CO. Accordingly, the peak at 1725 cm^{-1} in the untreated sample split into two peaks at 1698 and 1732 cm^{-1}, indicative of C=O groups in conjugated and unconjugated ketones/aldehydes.
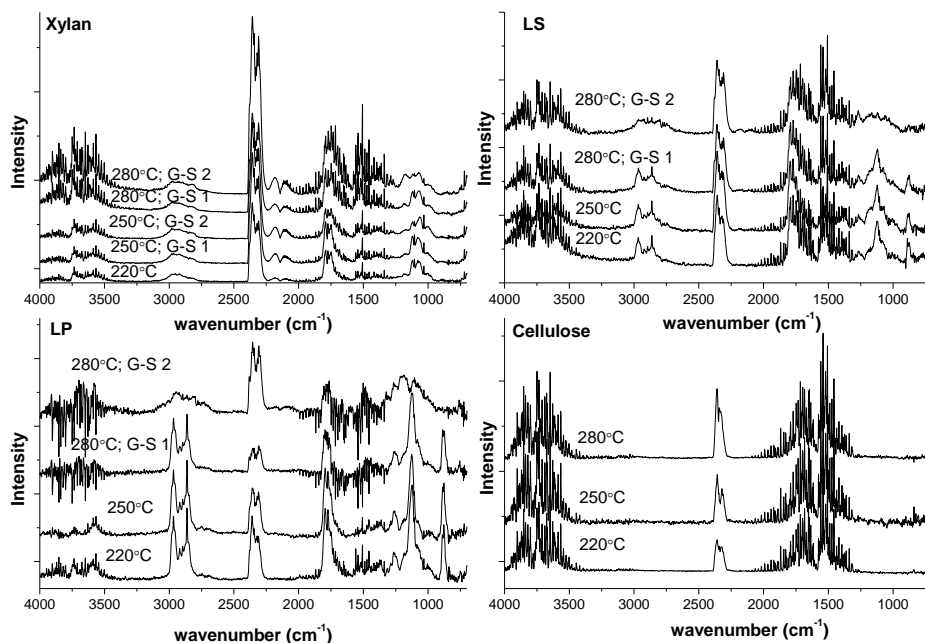

Fig. 2b. IR spectra obtained at the maximum evolution rate of corresponding 3D spectrograms of Fig. 2a. G-S 1 represents the spectrum from the first G-S peak, and G-S 2 represents the spectrum from the second G-S peak.

At 250 °C, the increase in peak intensity at 1732 and 1696 cm^{-1} was due to the decomposition of acetyl groups and the macromolecule fragments containing the xylan unit in the main chain, which did not decompose at low temperatures (Šimkovic *et al.* 1987). The presence of a new absorption peak at 1315 cm^{-1}, assigned to alkene C-H deformation vibration, suggests the formation of C=C groups, also evidenced by the increase in the stretching vibration of alkene C-H at 2975 cm^{-1}. These reactions occur at high temperatures, forming more C=C, C=O, and gas products similar to those at 220 °C, except for a trace of acetic acid. Moreover, the increase in the intensity of alkyl group peaks suggests that most carbonyl groups produced at high temperature remained in the solid phase.

With further torrefaction treatment at 280 °C, almost all characteristic peaks disappeared, contributing to notable releases of CO_2, CO, and acetic acid. The large absorptions of the solid residues at 1689, 1567, 1400, 1315, and 780 cm^{-1} suggest an abundance of unsaturated ketones, aldehydes, and carboxylic acid salts.
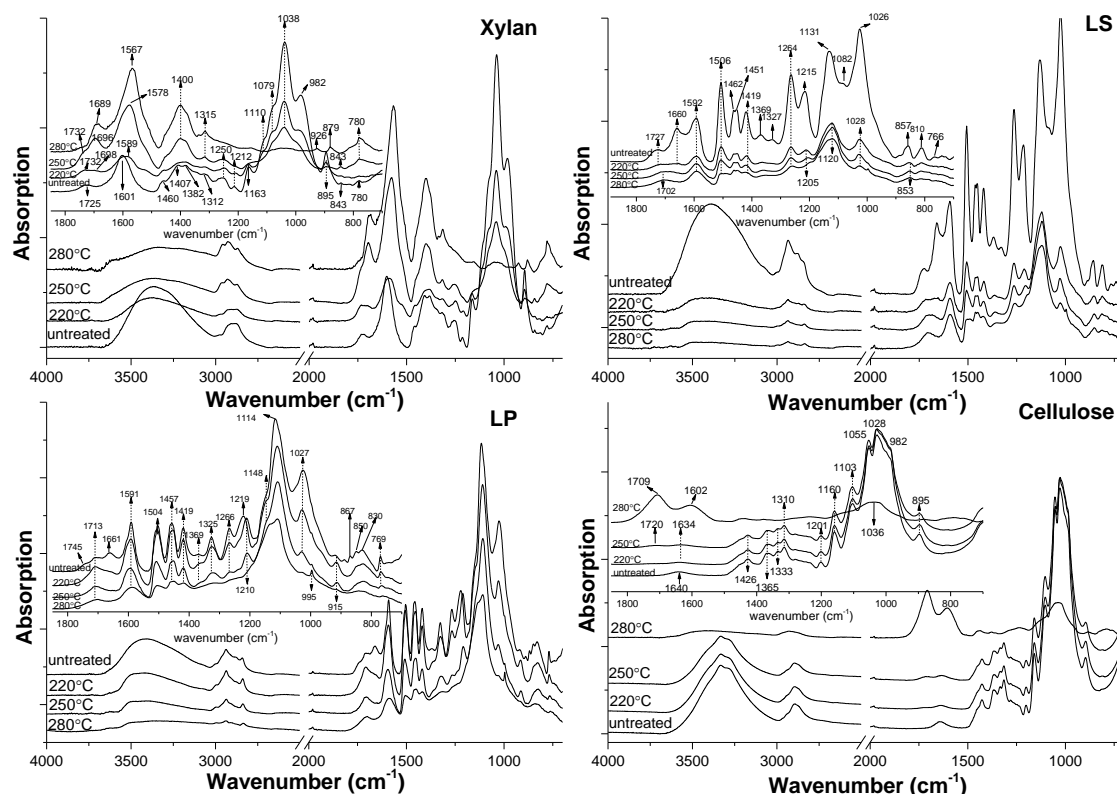

Fig. 3. FTIR-ATR spectra of torrefied and untreated samples

Lignin

Figure 1 shows that the two lignin samples decomposed rapidly during the first 10 min of treatment after the torrefaction temperature was reached, but thereafter, the rate of decomposition decreased. The first 10 min of treatment at 280 °C caused 20.5 and 29.6% mass losses of LS and LP, respectively, whereas only 8 and 10% additional mass losses occurred during the remainder of the torrefaction (Table 2, Fig. 1).

Unlike with xylan, increasing the temperature of the treatment did not increase the maximum intensity of the G-S peaks. The G-S peaks of both lignin samples were less intense at 280 °C, suggesting that the thermal degradation mechanism differed at the higher

temperature. Nevertheless, two successive G-S peaks from LS (the second peak was overlapped and presented as a shoulder) and LP appeared at 280 °C. This indicates that decomposition predominated at 220 and 250 °C but was suppressed by rearrangement at 280 °C, thereby reducing the evolution of volatiles and resulting in weaker G-S peaks.

As shown by FTIR gas analysis (Figs. 2a and 2b), absorptions of dioxane with four characteristic peaks at about 2968, 2865, 1125, and 880 cm^{-1} were detected at 220 and 250 °C and in the first G-S peak at 280 °C. This was due to the presence of residual dioxane used in the lignin preparation. This residual could have been the reason for the rapid mass loss of both lignin samples during the period immediately following drying. In addition to dioxane, water, CO_2, formic acid, acetic acid, methanol, and formaldehyde (2500 to 3200 cm^{-1}; 1600- to cm^{-1}) were the main volatiles identified following torrefaction of the two lignins. Moreover, a small amount of CO was found for both lignins at 280 °C. In addition, it should be noted that the emission of phenol (3600 to 3700 cm^{-1}; 2990 to 3150 cm^{-1}; 1420 to 1650 cm^{-1}; 900 to 1400 cm^{-1}) distinguished the gas spectrum of LP from that of LS.

Table 3. Dominant Volatiles under Various Torrefaction Conditions

Treatment		Dominant volatiles							
		H_2O	CO_2	CO	HCOOH	CH_3OH	CH_2O	CH_3COOH	phenol
Xylan	220 °C, 5 h	√	√	√	√	√			
	250 °C, 5h	√	√	√	√	√		√	
	280 °C, 5 h	√	√	√	√	√		√	
LS	220 °C, 5 h	√	√		√	√	√	√	
	250 °C, 5 h	√	√		√	√	√	√	
	280 °C, 5 h	√	√	√	√	√	√	√	
LP	220 °C, 5 h	√	√		√	√	√	√	
	250 °C, 5 h	√	√		√	√	√	√	
	280 °C, 5 h	√	√	√	√	√	√	√	√
Cellulose	220 °C, 5 h	√	√						
	250 °C, 5 h	√	√						
	280 °C, 5 h	√	√						

Lignin thermally decomposes over a broad temperature range because oxygen-containing functional groups such as phenols, methoxyls, aliphatic alcohols, carbonyls, and ethers have different thermal stabilities. In LS, absorption of O-H stretching vibrations and C-H stretching vibrations were notably diminished at 220 °C (Fig. 3), which is indicative of dehydration and dehydrogenation reactions. This is also evidenced by the drastic decline in the absorptions at 1082 and 1026 cm^{-1} (C-O stretch in secondary and primary alcohols, respectively) (Hergert 1960; Nada *et al.* 1998). Peaks at 1743 (C=O) and 766 cm^{-1} (O-C=O in-plane deformation) exhibited characteristics of esters and decreased with increasing temperature. Furthermore, dehydration/dehydrogenation resulted in the disappearance of the peak at 1660 cm^{-1}, which was attributed to the intra-molecular hydrogen-bond in carboxylic acid. Meanwhile, decreases in absorption peaks at 1462, 1451, and 1419 cm^{-1}, characteristic of asymmetric and symmetric CH_3 deformation in methoxy groups (Åkerholm and Salmén 2001; Nada *et al.* 1998), demonstrated the decomposition of the C_{aryl}-O-CH_3 group, the weakest bond in a guaiacol unit (Masuku *et al.* 1988). However, interpretation of the spectra was not straightforward because it is possible that the absorption peak at 1419 cm^{-1} was related to aromatic skeletal vibrations (Boeriu *et al.*

2004). Accordingly, this absorption peak was attributed to both types of vibrations (Faix 1991; Pandey 1999), although it was believed to be mostly due to C-H deformation vibrations in methoxy groups. The characteristic absorption of phenolic O-H deformation vibrations at 1215 cm^{-1} (Nada *et al.* 1998) also decreased with increasing temperature. Correspondingly, the decline of other characteristic phenolic absorptions at 1369 (Nada *et al.* 1998) and 1327 cm^{-1} (associated with ortho methoxy) (Bermello *et al.* 2002) are evidence of the decomposition of phenolic groups. Nevertheless, assignments of the peaks at 1369 and 1327 cm^{-1} was difficult in that the former was considered an aliphatic C-H stretch in CH$_3$ but not in methoxy (Faix 1991), while the latter was assigned to C-H bending of the methyl group in methoxy (Briggs *et al.* 1957). Because the intensity of the peak at 1369 cm^{-1} decreased remarkably and the peak at 1327 cm^{-1} nearly disappeared after treatment, the peak at 1369 cm^{-1} was attributed to phenolic OH combined with aliphatic C-H deformation vibrations, and the peak at 1327 cm^{-1} was attributed to C-H bending of the methyl group in methoxy. With the decomposition of the C$_{aryl}$-O-CH$_3$ group, the peak at 1215 cm^{-1} shifted to a lower wavenumber. In addition, the intensity of the asymmetric C-O-C stretching peak in aryl-alkyl ether at 1264 cm^{-1} (Briggs *et al.* 1957; Kotilainen *et al.* 2000) sharply decreased because of the poor thermal stability of the aryl-ether bonds, which undergo cleavage at low temperatures. Thus, the absorption intensities of all side groups in LS, including methoxy, aryl-alkyl ether, and phenolic OH, suggest that decomposition occurred during torrefaction at 220 °C.

The decomposition of the side groups caused the aromatic out-of-plane C-H deformation vibrations in 1,3,4-trisubstituted benzenes at 857 and 810 cm^{-1} (Hergert 1960; Boeriu *et al.* 2004) to decrease. Changes within the aromatic ring took place, as evidenced by the decrease in intensity of aromatic skeletal vibrations at 1592 and 1506 cm^{-1}. All characteristic absorptions were degraded further at 250 °C, and a small amount of CO was produced during torrefaction at 280 °C. A broad peak centered at 1702 cm^{-1} indicated the formation of conjugated carbonyls.

In LP, most absorption peaks were similar to those of LS, except for variations in intensities. Absorption of stretching O-H was weaker compared to that of LS, likely because hardwood lignin is composed of linear domains cross-linked though free phenolic groups. The pronounced peak at 1114 cm^{-1} was noticeably different in the spectra of the two lignins. Most studies assign this peak and the peak at 1131 cm^{-1} in LS to aromatic C-H in-plane deformation in S units in hardwood and G units in softwood, respectively. However, some investigators have proposed that these absorptions may be due to some other ether-type linkages (Briggs *et al.* 1957; Hergert 1960). This study suggests that both types of vibrations contribute to this peak. Moreover, the substitution pattern of LP was quite complex. A series of absorptions in the range of 867 to 830 cm^{-1} was detected, which was responsible for the aromatic C-H out-of-plane deformation vibrations. At 280 °C, the emission of phenol from LP also was observed.

In spite of its structural diversity, LP had similar thermal decomposition behaviour as LS, as shown by the cleavage of methoxyl groups in aryl-O-CH$_3$ and the cleavage of α, β-alkyl, and aryl ether units (Boeriu *et al.* 2004; Brosse *et al.* 2010).

Cellulose

Cellulose was extremely stable during torrefaction at 220 °C, losing only 3.5% of its mass after 5 h of treatment and 33.1% during torrefaction at 250 °C (Table 2; Fig. 1). A previous study showed that cellulose carbonises at low temperatures through dehydration and cross-linking reactions (Arseneau 1971), which may explain its stable behaviour at 220

and 250 °C. Unlike the thermal behaviour at 220 and 250 °C, cellulose slowly decomposed during the period following drying up until 10 min at 280 °C, resulting in 13.5% mass loss. However, it substantially deteriorated with prolonged treatment, resulting in 84.4% mass loss by the end of the torrefaction. Under these conditions, the cellulose was transformed from a crystalline structure to an amorphous structure and its cross-links were broken.

Figure 1 shows that the instantaneous concentration of the evolved gases from cellulose during torrefaction was disproportionally small relative to the corresponding mass loss rate. The fact that very small quantities of volatiles were detected during the torrefaction of cellulose is likely due to the temperature of the heated transfer line connecting the TGA to the FTIR, which prevented the detection of compounds with higher boiling points than the torrefaction temperature. Based on the obtained gas FTIR (see Figs. 2a and 2b), the characteristic bands of cellulose revealed the production of water and CO_2.

Because of the aforementioned difficulties in detecting certain gaseous products, it was especially worthwhile to study the changes that occurred in the solid phase. For untreated cellulose (Fig. 3), an absorption peak centered at 1640 cm^{-1} in the spectrum was observed. As it is well known that cellulose is rich in hydroxyl groups that are prone to absorb moisture, it is likely that H_2O was responsible for this peak (Pandey 1999). Peaks at around 3300 (v OH), around 2890 (v CH$_2$; v CH), 1426 (ρ CH$_2$, sym.), 1365 (δ CH), 1333 (δ CH in-plane), 1310 (δ CH; δ OH), 1201 (ρ OH; δ CH), 1160 (v C-O-C in bridge, asym.), 1103 (ring valence vibration, asym.), 1055 (v O-C-O, alicyclic secondary alcohols), 1028 (v C-O in primary alcohols), 982 (δ OH, ring), and 895 cm^{-1} (v C-O-C in bridge, sym.) were typical characteristic absorptions for cellulose (Blackwell 1977; Fengel and Ludwig 1991). At 220 °C, cellulose cross-linked and dehydrated, creating a new peak at 1634 cm^{-1} characteristic of C=C absorption. Another weak peak arising at 1720 cm^{-1} during treatment at 250 °C was attributed to C=O absorption, indicating the formation of ketones or aldehydes.

Remarkable dehydration, cleavage, and rearrangement of cellulose occurred during treatment at 280 °C. All characteristic absorptions nearly vanished, leaving three distinct absorption peaks at 1709, 1602, and 1036 cm^{-1}, assigned to conjugated C=O, C=C-C=C, and C-O bonds, respectively (Lv *et al.* 2012). These results revealed that dehydration and decarbonation were predominant and accounted for over 33% of the mass losses up to 250 °C, while cleavage and rearrangement prevailed at 280 °C.

CONCLUSIONS

1. Cellulose is known to be extremely thermally stable. However, this behavior is valid only at short terms, and this trend is inverted over long time-duration, resulting in much more mass losses than all the other components.

2. Analysis of gaseous volatiles from each sample at different torrefaction temperatures showed similar characteristic bands, implying that the effects of temperature and duration on gas products vary primarily in the amounts, rather than the types, of volatiles produced. Therefore, shorter residence time at higher temperature can be applied for the equivalent treatment intensity.

3. This continuous measurement over long residence times in isothermal conditions is essential to predict the treatment of large quantities of biomass in thick beds, which are difficult to heat up and cool down. Together with the exothermic reactions, the actual

residence time of particles under treatment is longer, resulting in different chemical pathways over wide ranges of temperature and time-durations.

4. Results of this study are essential to supply modelling tools at large scale with robust kinetics. This allows simulations to be predictive whatever the configuration and to serve for innovation and process improvement at industrial scale.

ACKNOWLEDGMENTS

REFERENCES CITED

Åkerholm, M., and Salmén, L. (2001). "Interactions between wood polymers studied by dynamic FT-IR spectroscopy," *Polymer* 42(3), 963-969. DOI: 10.1016/S0032-3861(00)00434-1

Arseneau, D. F. (1971). "Competitive reaction in the thermal decomposition of cellulose," *Can. J. Chem.* 49(4), 632-638. DOI: 10.1139/v71-101

Bermello, A., Del Valle, M., Orea, U., and Carballo, L. R. (2002). "Characterization by infrared spectroscopy of lignins of three eucalyptus species," *Int. J. Polym. Mater.* 51(6), 557-566. DOI: 10.1080/00914030209696301

Biagini, E., Barontini, F., and Tognotti, L. (2006). "Devolatilization of biomass fuels and biomass components studied by TGA/FTIR technique," *Ind. Eng. Chem. Res.* 45(13), 4486-4493. DOI: 10.1021/ie0514049

Blackwell, J. (1977). "Infrared and Raman spectroscopy of cellulose," in: *Cellulose Chemistry and Technology*, J. C. Arthur (ed.), American Chemical Society, Washington, DC. DOI: 10.1021/bk-1977-0048.ch014

Boeriu, C. G., Bravo, D., Gosselink, R. J. A., and van Dam, J. E. G. (2004). "Characterisation of structure-dependent functional properties of lignin with infrared spectroscopy," *Ind. Crops Prod.* 20(2), 205-218. DOI: 10.1016/j.indcrop.2004.04.022

Briggs, L. H., Colebrook, L. D., Fales, H. M., and Wildman, W. C. (1957). "Infrared absorption spectra of methylenedioxy and aryl ether groups," *Anal. Chem.* 29(6), 904-911. DOI: 10.1021/ac60126a014

Brosse, N., Hage, R. E. I., Chaouch, M., Pétrissans, M., Dumarçay, S., and Gérardin, P. (2010). "Investigation of the chemical modifications of beech wood lignin during heat treatment," *Polym. Degrad. Stab.* 95(9), 1721-1726. DOI: 10.1016/j.polymdegradstab.2010.05.018

Buslov, D. K., Kaputski, F. N., Sushko, N. I., Torgashev, V. I., Solov'eva, L. V., Tsarenkov, V. M., Zubets, O. V., and Larchenko, L. V. (2009). "Infrared spectroscopic analysis of the structure of xylans," *J. Appl. Spectrosc.* 76(6), 801-805. DOI: 10.1007/s10812-010-9282-z

Cavagnol, S., Roesler, J. F., Sanz, E., Nastoll, W., Lu, P., and Perré, P. (2015). "Exothermicity in wood torrefaction and its impact on product mass yields: From micro to pilot scale," *Can. J. Chem. Eng.* 93(2), 331-339. DOI: 10.1002/cjce.22128

Di Blasi, C., and Lanzetta, M. (1997). "Intrinsic kinetics of isothermal xylan degradation in inert atmosphere," *J. Anal. Appl. Pyrolysis* 40(4), 287-303. DOI: 10.1016/S0165-2370(97)00028-4

Faix, O. (1991). "Classification of lignins from different botanical origins by FT-IR spectroscopy," *Holzforschung* 45(s1), 21-27. DOI: 10.1515/hfsg.1991.45.s1.21

Fengel, D., and Ludwig, M. (1991). "Possibilities and limits of the FTIR spectroscopy for the characterization of cellulose. 1. Comparison of various cellulose fibers and bacteria cellulose," *Papier* 45(2), 45-51.

Hergert, H. L. (1960). "Infrared spectra of lignin and related compounds. II. Conifer lignin and model compounds," *J. Org. Chem.* 25(3), 405-413. DOI: 10.1021/jo01073a026

Kačuráková, M., Wellner, N., Ebringerová, A., Hromádková, Z., Wilson, R. H., and Belton, P. S. (1999). "Characterisation of xylan-type polysaccharides and associated cell wall components by FT-IR and FT-Raman spectroscopies," *Food Hydrocolloid.* 13(1), 35-41. DOI: 10.1016/S0268-005X(98)00067-8

Kotilainen, R. A., Toivanen, T. J., and Alén, R. J. (2000). "FT-IR monitoring of chemical changes in softwood during heating," *J. Wood. Chem. Technol.* 20(3), 307-320. DOI: 10.1080/02773810009349638

Lapierre, C., Monties, B., and Rolando, C. (1986). "Thioacidolysis of poplar lignins - Identification of monomeric syringyl products and characterization of guaiacyl-syringyl lignin fractions," *Holzforschung* 40(2), 113-118. DOI: 10.1515/hfsg.1986.40.2.113

Lv, P., Almeida, G., and Perré, P. (2012). "Torrefaction of cellulose: Validity and limitation of the temperature/duration equivalence," *BioResources* 7(3), 3720-3731. DOI: 10.15376/biores.7.3.3720-3731

Marchessault, R. H., and Liang, C. Y. (1962). "The infrared spectra of crystalline polysaccharides VIII xylans," *J. Polym. Sci.* 59(168), 357-378. DOI: 10.1002/pol.1962.1205916813

Masuku, C. P., Vuori, A., and Bredenberg, J. B.-son. (1988). "Thermal reactions of the bonds in lignin: I. Thermolysis of 4-propylguaiacol," *Holzforschung* 42(6), 361-367. DOI: 10.1515/hfsg.1988.42.6.361

Nada, A. A. M. A., El-Sakhawy, M., and Kamel, S. M. (1998). "Infra-red spectroscopic study of lignins," *Polym. Degrad. Stab.* 60(2-3), 247-251. DOI: 10.1016/S0141-3910(97)00072-4

Pandey, K. K. (1999). "A study of chemical structure of soft and hardwood and wood polymers by FTIR spectroscopy," *J. Appl. Polym. Sci.* 71(12), 1969-1975. DOI: 10.1002/(SICI)1097-4628(19990321)71:12<1969::AID-APP6>3.0.CO;2-D

Qu, T. T., Guo, W. J., Shen, L. H., Xiao, J., and Zhao, K. (2011). "Experimental study of biomass pyrolysis based on three major components: Hemicellulose, cellulose and lignin," *Ind. Eng. Chem. Res.* 50(18), 10424-10433. DOI: 10.1021/ie1025453

Rousset, P., Lapierre, C., Pollet, B., Quirino, W., and Perré, P. (2009). "Effect of severe thermal treatment on spruce and beech wood lignins," *Ann. For. Sci.* 66(1), 110. DOI: 10.1051/forest/2008078

Rousset, P., Davrieux, F., Macedo, L., and Perré, P. (2011). "Characterisation of the torrefaction of beech wood using NIRS: Combined effects of temperature and

bioresources.com

duration," *Biomass Bioenerg.* 35(3), 1219-1226. DOI: 10.1016/j.biombioe.2010.12.012

Shen, D. K., and Gu, S. (2009). "The mechanism for thermal decomposition of cellulose and its main products," *Bioresour. Technol.* 100(24), 6496-504. DOI: 10.1016/j.biortech.2009.06.095

Shen, D. K., Gu, S., Luo, K. H., Wang, S. R., and Fang, M. X. (2010a). "The pyrolytic degradation of wood-derived lignin from pulping process," *Bioresour. Technol.* 101(15), 6136-6146. DOI: 10.1016/j.biortech.2010.02.078

Shen, D. K., Gu, S., and Bridgwater, A. V. (2010b). "Study on the pyrolytic behaviour of xylan-based hemicellulose using TGA–FTIR and Py–GC–FTIR," *J. Anal. Appl. Pyrolysis* 87(2), 199-206. DOI: 10.1016/j.jaap.2009.12.001

Shevchenko, L. L. (1963). "Infrared spectra of salts and complexes of carboxylic acids and some of their derivatives," *Russ. Chem. Rev.* 32(4), 201-207. DOI: 10.1070/RC1963v032n04ABEH001329

Šimkovic, I., Hirsch, J. Ebringerová, A., and Königstein, J. (1987). "Thermal degradation of model compounds with blocked hemiacetal group related to (4-O-methyl-D-glucurono)-D-xylan," *J. Appl. Polym. Sci.* 33(5), 1473-1477. DOI: 10.1002/app.1987.070330503

Wu, Y. M., Zhao, Z. L., Li, H. B., and He, F. (2009). "Low temperature pyrolysis characteristics of major components of biomass," *J. Fuel. Chem. Technol.* 37(4), 427-432. DOI: 10.1016/S1872-5813(10)60002-3

Yang, H. P., Yan, R., Chen, H., Lee, D., and Zheng, C. (2007). "Characteristics of hemicellulose, cellulose and lignin pyrolysis," *Fuel* 86(12-13), 1781-1788. DOI: 10.1016/j.fuel.2006.12.013